arXiv:1507.05124v1 [quant-ph] 17 Jul 2015

Rabi oscillations in two-level systems beyond the rotating-wave approximation

Adriano A. Batista*

Departamento de Física

Universidade Federal de Campina Grande

Campina Grande-PB

CEP: 58109-970

Brazil

(Dated: March 3, 2022)

Abstract

Here we use perturbation techniques based on the averaging method to investigate Rabi oscillations in cw and pulse-driven two-level systems (TLS's). By going beyond the rotating-wave approximation, especifically to second-order in perturbation, we obtain the Bloch-Siegert shift of the TLS resonant frequency, in which the resonant frequency increases with the driving field amplitude. This frequency shift implies that short resonant π-pulses in which the Rabi frequency is approximately 40% or higher of the transition frequency do not achieve complete inversion in TLS's. Hence, guided by analytical results based on the averaging technique, we propose two methods for obtaining population inversions in the TLS driven by short π-pulses: one with chirping and the other with pulse shaping and near resonance blue-shifted detuning. Both methods minimize dephasing due to the Bloch-Siegert shift, reduce the dependance of the excitation of the TLS on the pulse phase, and are very effective in achieving complete population inversions.

* adriano@df.ufcg.edu.br

I. INTRODUCTION

Here we investigate the coherent, cw or pulsed, excitation of two-level systems (TLS's) in quantum mechanics, under the semiclassical approximation. Our main purpose is to develop approximate analytical methods with better precision than the rotating-wave approximation (RWA) that will help us in designing more accurate and faster coherent control schemes than what is currently available in the literature.

We use the perturbative method known as the averaging method [1, 2] to go one step beyond RWA. Usually this method is applied to periodically-driven dynamical systems with two very different time scales (one fast and the other slow), although, as we will see, even when the time scales are not very far apart the method is still very useful. Furthermore, this method has the added advantage that it can provide efficiently both transient and stationary approximate solutions, unlike the usual time-dependent perturbative methods of quantum mechanics. The proposed approach is considerably simpler than to implement than Floquet theory [3, 4], which technically is not applicable to TLS's excited by pulses. By implementing our method, we obtained the first correction to the resonant frequency of the TLS as the pump amplitude is increased, an effect known as the Bloch-Siegert shift [5].

Quantum control of population transfer in TLS's is a topic of intense current theoretical and experimental investigations [6–9], mostly with the purpose of implementing quantum gates in various physical systems for quantum computing. Hence, it is desirable that laser pulses used in the realization of quantum gates be as short in time as possible so that they conform with basic theoretical models of quantum computing [10]. Furthermore, such short pulses reduce the adverse effect of decoherence, which then reduce the amount of errors involved in computation with qubits. On the other hand, the fields become stronger, the Fourier spectrum widens, and the control becomes more difficult, with the breaking up of the RWA and, consequently,

of the area theorem [11–13], which depends on the RWA. In such situations, the effectiveness of short and high-amplitude π-pulses depends on the phase of the pulse as well. Hence, in order to diminish such difficulties, we designed π-pulses, either with chirp in the carrier frequency or with pulse shaping with near resonance blue-shifted carrier frequency that minimizes the dephasing effects due to Bloch-Siegert shift. Analytical and numerical results of this approach of pulse chirping or shaping are presented with π-pulse-driven TLS's that yield considerably deeper interlevel population transfers and have almost no dependance on the phase of the pulses. This adds to recent investigations on quantum control of TLS's that try to achieve maximum population transfer either with chirping, which mostly use linearly-chirped pulses [14–16] or with pulse shaping [17].

This paper is organized as follows. In Sec. II, we review the results of RWA for the Schrödinger equation for the ac-driven TLS and present a naive perturbation method for tentatively going beyond RWA. In Sec. III, we obtain the 2nd-order averaging method correction to the RWA time-evolution. In Sec. IV, we obtain the density-matrix equations of motion in the 2nd-order averaging approximation. In Sec. V, we apply our theoretical results in the design of effective π-pulses. In Sec. VI, we discuss possible applications of our main results and draw our conclusions.

II. RABI OSCILLATIONS IN A TWO-LEVEL SYSTEM

The problem of coherent control of TLS's has a long and intense history, dating back to the 30's. It started with the study of the dynamics of magnetization of nuclei with spin 1/2 interacting with a magnetic field $\vec{B}(t) = \vec{B}_{dc} + \vec{B}_{ac}\cos(\omega t)$, in which there is an angle between the dc and ac components of the magnetic field. This was originally investigated and solved in the RWA, in a semiclassical approach, by I. Rabi in Ref. [18]. He found that, in resonance, there is a precession of the magnetization

around the ac field, which became known as Rabi cycle, at a frequency $g\mu_B B_{ac}/\hbar$, known as Rabi frequency, in which g is the gyromagnetic constant and μ_B is the Bohr magneton. This system has been found to have a time evolution equivalent to that of a TLS (atom, molecule, quantum dot, exciton, etc) interacting with a single mode of the electromagnetic field inside an optical cavity.

This generic Hamiltonian for this dynamical system can be written as

$$\mathcal{H}(t) = E_1|1\rangle\langle 1| + E_2|2\rangle\langle 2| + 2\hbar\Omega_0\cos(\omega t)\left[|1\rangle\langle 2| + |2\rangle\langle 1|\right]. \tag{1}$$

The wave function in the two-level approximation is given by

$$|\psi(t)\rangle = C_1(t)|1\rangle + C_2(t)|2\rangle.$$

Hence, the corresponding Schrödinger equation is

$$\imath\hbar\dot{C}_1 = E_1C_1 + 2\hbar\Omega_0\cos(\omega t)C_2, \tag{2a}$$

$$\imath\hbar\dot{C}_2 = E_2C_2 + 2\hbar\Omega_0\cos(\omega t)C_1. \tag{2b}$$

With the transformations $C_1(t) = e^{-\frac{\imath E_1}{\hbar}t}c_1(t)$ and $C_2(t) = e^{-\frac{\imath E_2}{\hbar}t}c_2(t)$, we obtain the interaction picture dynamics, which is given by

$$\imath\dot{c}_1 = 2\Omega_0 e^{-i\omega_0 t}\cos(\omega t)c_2 = \Omega_0 e^{\imath\delta t}\left(1 + e^{-2\imath\omega t}\right)c_2, \tag{3a}$$

$$\imath\dot{c}_2 = 2\Omega_0 e^{i\omega_0 t}\cos(\omega t)c_1 = \Omega_0 e^{-\imath\delta t}\left(1 + e^{2\imath\omega t}\right)c_1, \tag{3b}$$

where $\omega_0 = \frac{E_2 - E_1}{\hbar}$ is the transition frequency and $\delta = \omega - \omega_0$ is the detuning. In general this system would be quasiperiodically driven, and thus one could not readily apply the averaging method or Floquet theory. One fixes this problem with the following transformation

$$c_1(t) = e^{\frac{\imath\delta t}{2}}b_1(t), \tag{4a}$$

$$c_2(t) = e^{-\frac{\imath\delta t}{2}}b_2(t), \tag{4b}$$

we obtain the equations of motion

$$\imath\dot{b}_1 = \frac{\delta}{2}b_1 + \Omega_0\left(1 + e^{-2\imath\omega t}\right)b_2, \tag{5a}$$

$$\imath\dot{b}_2 = -\frac{\delta}{2}b_2 + \Omega_0\left(1 + e^{2\imath\omega t}\right)b_1, \tag{5b}$$

which are a parametrically-driven dynamical system with periodic coefficients. Hence, we can now perform the usual RWA and obtain

$$\imath\dot{b}_1 = \frac{\delta}{2}b_1 + \Omega_0 b_2, \tag{6}$$

$$\imath\dot{b}_2 = -\frac{\delta}{2}b_2 + \Omega_0 b_1. \tag{7}$$

For this approximation to be valid, we assume δ and $\Omega_0 = \mathcal{O}(\epsilon)$, with $0 < \epsilon << 1$. With a few algebraic steps one finds

$$\ddot{b}_i = -\left(\Omega_0^2 + \frac{\delta^2}{4}\right)b_i,$$

where $i = 1, 2$. For the initial values $C_1(0) = b_1(0) = 1$ and $C_2(0) = b_2(0) = 0$, which are equivalent to $b_1(0) = 1$ and $\dot{b}_1(0) = -\imath\delta/2$ or to $b_2(0) = 0$ and $\dot{b}_2(0) = -\imath\Omega_0$ we have

$$b_1(t) = \cos(\Omega t) - \frac{\imath\delta}{2\Omega}\sin(\Omega t), \tag{8a}$$

$$b_2(t) = -\frac{\imath\Omega_0}{\Omega}\sin(\Omega t), \tag{8b}$$

where $\Omega = \sqrt{\Omega_0^2 + \frac{\delta^2}{4}}$. Hence the occupation probabilities in each level are

$$|C_1(t)|^2 = \cos^2(\Omega t) + \frac{\delta^2}{4\Omega^2}\sin^2(\Omega t), \tag{9a}$$

$$|C_2(t)|^2 = \frac{\Omega_0^2}{\Omega^2}\sin^2(\Omega t). \tag{9b}$$

In Fig. 1, we compare the ground state occupation probability (population) evolution from the numerical integration of Eq.(2) with the corresponding population evolution given by RWA in Eqs. (9). The numerical integrator used was Python's Scipy odeint with a time step of 2^{-10}. One sees that there is considerable dephasing between the RWA and numerical integration results. In order to reduce this type of problem, one has to go beyond the RWA. One could attempt to achieve that by simply replacing the RWA solution, given in Eqs.(8), and using the transformation (4) backwards, in the right hand of Eq.(3). We obtain

$$c_1(t) = 1 - 2\imath\Omega_0 \int_0^t e^{-i\omega_0 s}\cos(\omega s)e^{-i\delta s/2}b_2(s)ds \tag{10a}$$

$$= 1 - \frac{2\Omega_0^2}{\Omega}\int_0^t e^{-i(\omega_0+\delta/2)s}\cos(\omega s)\sin(\Omega s)ds \tag{10b}$$

$$= 1 - \frac{\Omega_0^2}{\Omega}\int_0^t e^{-i(\omega_0+\delta/2)s}\left\{\sin[(\omega+\Omega)s] + \sin[(\Omega-\omega)s]\right\}ds. \tag{10c}$$

We need to find the integrals

$$\int_0^t e^{-i(\omega_0+\delta/2)s}\sin[(\Omega+\omega)s]ds = -\frac{e^{i(\Omega+\delta/2)t}-1}{2\Omega+\delta}$$
$$-\frac{e^{-i(\Omega+2\omega-\delta/2)t}-1}{2\Omega+4\omega-\delta}, \tag{11}$$

$$\int_0^t e^{-i(\omega_0+\delta/2)s}\sin[(\Omega-\omega)s]ds = \frac{-e^{i(\Omega-2\omega+\delta/2)t}+1}{2\Omega-4\omega+\delta}$$
$$-\frac{e^{-i(\Omega-\delta/2)t}-1}{2\Omega-\delta}. \tag{12}$$

This simple procedure fails to achieve more accurate results than the RWA, though, as one can see in Fig. 2, since it does not decrease the dephasing problem of the RWA. Another approach has to be devised in order to give a better approximation than the RWA to the Rabi oscillations without too much burden. Since the RWA is equivalent to the averaging method in the 1st-order approximation, a natural candidate to achieve better results than the RWA is the averaging method to second order. That is what is accomplished in the next section.

III. RABI OSCILLATIONS USING THE AVERAGING METHOD TO SECOND ORDER

Although one could apply Floquet theory to solve the system of differential equations (5) exactly, such as was performed in Refs. [3, 4], here, instead, we will use the simpler approach of going just one step further than the RWA in solving this system approximately using the averaging method to second order [1, 19].

Using the notation of Ref. [19], we have

$$\tilde{f}(y,t) = -\imath\Omega_0 \begin{bmatrix} 0 & e^{-2\imath\omega t} \\ e^{2\imath\omega t} & 0 \end{bmatrix} \begin{bmatrix} y_1 \\ y_2 \end{bmatrix},$$

with the weakly nonlinear transformation $b(t) = y(t) + \epsilon\mathcal{W}(y,t)$, with $b(t), y(t) \in \mathbb{C}^2$, where $\mathcal{W}(y,t)$ obeys the differential equation

$$\mathcal{W}_t = \tilde{f}. \tag{13}$$

Hence, upon integration of Eq. (13), we obtain

$$\begin{aligned} \epsilon\mathcal{W}(y,t) &= \frac{\Omega_0}{2\omega} \begin{bmatrix} 0 & e^{-2\imath\omega t} \\ -e^{2\imath\omega t} & 0 \end{bmatrix} \begin{bmatrix} y_1 \\ y_2 \end{bmatrix} \\ &= \frac{\Omega_0}{2\omega} \begin{bmatrix} e^{-2\imath\omega t} y_2 \\ -e^{2\imath\omega t} y_1 \end{bmatrix}, \end{aligned} \tag{14}$$

in which the constants of integration were set to zero. The Jacobian matrix of $\tilde{f}$ is

$$\epsilon D\tilde{f} = -\imath\Omega_0 \begin{bmatrix} 0 & e^{-2\imath\omega t} \\ e^{2\imath\omega t} & 0 \end{bmatrix}.$$

With another weakly nonlinear transformation $y(t) = z(t) + \epsilon^2 v(z,t)$, we obtain the second-order averaged system, corresponding to the original nonautonomous ordinary differential equation (ODE) system of Eq. (5),

$$\dot{z} = \epsilon f_0(z) + \epsilon^2 \overline{D\tilde{f}\mathcal{W}},$$

where the overline denotes the time averaging. We then find

$$\epsilon^2 \overline{D\tilde{f}\mathcal{W}} = -\frac{\imath\Omega_0^2}{2\omega} \begin{bmatrix} -1 & 0 \\ 0 & 1 \end{bmatrix} \begin{bmatrix} z_1 \\ z_2 \end{bmatrix}.$$

Consequently, we find

$$\begin{aligned} \begin{bmatrix} \dot{z}_1 \\ \dot{z}_2 \end{bmatrix} &= -\imath \begin{bmatrix} \frac{\delta}{2} & \Omega_0 \\ \Omega_0 & -\frac{\delta}{2} \end{bmatrix} \begin{bmatrix} z_1 \\ z_2 \end{bmatrix} - \frac{\imath\Omega_0^2}{2\omega} \begin{bmatrix} -1 & 0 \\ 0 & 1 \end{bmatrix} \begin{bmatrix} z_1 \\ z_2 \end{bmatrix} \\ &= -\imath \begin{bmatrix} \frac{\tilde{\delta}}{2} & \Omega_0 \\ \Omega_0 & -\frac{\tilde{\delta}}{2} \end{bmatrix} \begin{bmatrix} z_1 \\ z_2 \end{bmatrix}, \end{aligned} \tag{15}$$

where $\tilde{\delta} = \delta - \frac{\Omega_0^2}{\omega}$. One sees that the Eqs.(15) have the same form as the Eqs. (7), with the correction for the detuning. This correction reduces the dephasing of the usual RWA for the Rabi oscillations. This shift in resonant frequency relative to the RWA resonant frequency is known as the Bloch-Siegert shift [3, 5]. That is not all though, the initial values of the ODE system (15) are different from the initial values of Eqs. (7). Hence, that implies that the solution of Eq. (15) is given by

$$z_1(t) = A_1 \cos(\tilde{\Omega}t) + B_1 \sin(\tilde{\Omega}t), \tag{16a}$$

$$z_2(t) = A_2 \cos(\tilde{\Omega}t) + B_2 \sin(\tilde{\Omega}t), \tag{16b}$$

where the coefficients can be found from the initial values

$$z_1(0) = A_1 = \frac{1}{1 + \left(\frac{\Omega_0}{2\omega}\right)^2}, \tag{17}$$

$$z_2(0) = A_2 = \frac{\Omega_0/(2\omega)}{1 + \left(\frac{\Omega_0}{2\omega}\right)^2}, \tag{18}$$

$$\dot{z}_1(0) = \tilde{\Omega}B_1 = -\frac{\imath}{2}\left[\tilde{\delta}z_1(0) + 2\Omega_0 z_2(0)\right], \tag{19}$$

$$\dot{z}_2(0) = \tilde{\Omega}B_2 = -\frac{\imath}{2}\left[2\Omega_0 z_1(0) - \tilde{\delta}z_2(0)\right]. \tag{20}$$

IV. THE DENSITY MATRIX EQUATIONS OF MOTION

In order to investigate one qubit dynamics with depopulation and decoherence effects, one has to use the density-matrix equations of motion, instead of the Schrödinger equation. We start with the following equations

$$\dot{\Delta} = -\gamma_1(\Delta - \Delta_0) + 4\mathrm{Im}\,\sigma F(t), \tag{21a}$$

$$\dot{\sigma} = -\gamma_2\sigma + \imath\omega_0\sigma - \imath\Delta F(t), \tag{21b}$$

where $F(t) = 2\Omega_0\cos(\omega t+\varphi_0)$, Δ is the population difference $N_1(t)-N_2(t)$, Δ_0 is the equilibrium population difference, and $\sigma(t)$ is the off-diagonal element $\rho_{21}(t)$ of the density matrix in the basis of the two states $|1\rangle$ and $|2\rangle$. The parameters $\gamma_1 = 1/T_1$, the depopulation rate, and $\gamma_2 = 1/T_2$, the decoherence rate, are dissipation rates obtained from the relaxation-time approximation. We now proceed to implement the averaging method with the transformation $\sigma(t) = e^{\imath\omega t}\tilde{\sigma}(t)$ to set the Eqs. (21) in the slowly-varying frame (also known as the interaction representation). Hence, we obtain

$$\dot{\Delta} = -\gamma_1(\Delta - \Delta_0) - 2\imath\Omega_0\left(\tilde{\sigma}e^{\imath\omega t} - \tilde{\sigma}^* e^{-\imath\omega t}\right)\left(e^{\imath(\omega t+\varphi_0)} + e^{-\imath(\omega t+\varphi_0)}\right), \tag{22a}$$

$$\dot{\tilde{\sigma}} = -\gamma_2\tilde{\sigma} - \imath\delta\tilde{\sigma} - \imath\Omega_0\Delta\left[e^{\imath\varphi_0} + e^{-\imath(2\omega t+\varphi_0)}\right], \tag{22b}$$

$$\dot{\tilde{\sigma}}^* = -\gamma_2\tilde{\sigma}^* + \imath\delta\tilde{\sigma}^* + \imath\Omega_0\Delta\left[e^{-\imath\varphi_0} + e^{\imath(2\omega t+\varphi_0)}\right], \tag{22c}$$

where we included the equation for $\dot{\tilde{\sigma}}^*$, because it will be used lates in the averaging method to second order. Doing 1st-order averaging, which is equivalent to the RWA, we obtain

$$\dot{\Delta} = -\gamma_1(\Delta - \Delta_0) - 2\imath\Omega_0\left[\tilde{\sigma}e^{-\imath\varphi_0} - \tilde{\sigma}^* e^{\imath\varphi_0}\right], \tag{23a}$$

$$\dot{\tilde{\sigma}} = -\gamma_2\tilde{\sigma} - \imath\delta\tilde{\sigma} - \imath\Omega_0\Delta e^{\imath\varphi_0}, \tag{23b}$$

whose fixed-point solutions are given by

$$\tilde{\sigma} = -\frac{\imath\Omega_0\Delta e^{\imath\varphi_0}}{\gamma_2 + \imath\delta} = -\frac{\imath\Omega_0\Delta_0(\gamma_2 - \imath\delta)e^{\imath\varphi_0}}{\gamma_2^2 + \delta^2 + 4\Omega_0^2\gamma_2/\gamma_1}, \tag{24}$$

$$\Delta = \frac{\Delta_0}{1 + \dfrac{4\Omega_0^2\gamma_2}{\gamma_1(\gamma_2^2 + \delta^2)}}. \tag{25}$$

Next, we proceed to the calculations for the 2nd-order averaging corrections in the dynamics of the Bloch equations.

A. Averaging to 2nd-order

Again using the notation of Ref. [19] we obtain

$$\epsilon\tilde{f} = -\imath\Omega_0 \begin{bmatrix} 2\left(\tilde{\sigma}e^{\imath(2\omega t+\varphi_0)} - \tilde{\sigma}^* e^{-\imath(2\omega t+\varphi_0)}\right) \\ \Delta e^{-\imath(2\omega t+\varphi_0)} \\ -\Delta e^{\imath(2\omega t+\varphi_0)} \end{bmatrix}$$

with the weakly nonlinear transformation $b(t) = y(t) + \epsilon\mathcal{W}(y,t)$, with $b(t), y(t) \in \mathbb{C}^3$, where $\mathcal{W}(y,t)$ obeys the differential equation

$$\mathcal{W}_t = \tilde{f}. \tag{26}$$

Hence, upon integration of Eq. (26), we obtain

$$\epsilon\mathcal{W}(y,t) = -\frac{\Omega_0}{2\omega} \begin{bmatrix} 2\left(\tilde{\sigma}e^{\imath(2\omega t+\varphi_0)} + \tilde{\sigma}^* e^{-\imath(2\omega t+\varphi_0)}\right) \\ -\Delta e^{-\imath(2\omega t+\varphi_0)} \\ -\Delta e^{\imath(2\omega t+\varphi_0)} \end{bmatrix}, \tag{27}$$

in which the constants of integration were set to zero. The Jacobian matrix of $\tilde{f}$ is

$$\epsilon D\tilde{f} = -\imath\Omega_0 \begin{bmatrix} 0 & 2e^{\imath(2\omega t+\varphi_0)} & -2e^{-\imath(2\omega t+\varphi_0)} \\ e^{-\imath(2\omega t+\varphi_0)} & 0 & 0 \\ -e^{\imath(2\omega t+\varphi_0)} & 0 & 0 \end{bmatrix}$$

$$\epsilon^2 \overline{D\tilde{f}\mathcal{W}} = \frac{\imath\Omega_0^2}{\omega} \begin{bmatrix} 0 \\ \tilde{\sigma} \\ -\tilde{\sigma}^* \end{bmatrix}.$$

Hence, in the second-order averaging we obtain

$$\dot{\Delta} = -\gamma_1(\Delta - \Delta_0) - 2\imath\Omega_0 \left[\tilde{\sigma} e^{-\imath\varphi_0} - \tilde{\sigma}^* e^{\imath\varphi_0}\right], \tag{28a}$$

$$\dot{\tilde{\sigma}} = -\gamma_2\tilde{\sigma} - \imath\left(\delta - \frac{\Omega_0^2}{\omega}\right)\tilde{\sigma} - \imath\Omega_0\Delta e^{\imath\varphi_0}. \tag{28b}$$

One can readily see that in this approximation the driving phase has no effect on the population dynamics, and just adds a constant phase to $\tilde{\sigma}$.

V. APPLICATION TO QUANTUM CONTROL

We now proceed to apply the averaging method to study the action of pulses on the dynamics of TLS's. In particular, we are interested in designing π-pulses to accomplish the deepest population inversions. By examining Eq. (28), one sees that the usual area theorem [11–13] does not work. A pulse with central frequency at $\omega = \omega_0$ loses resonance as the pulse amplitude increases and, consequently, if the peak amplitude is large enough, there is substantial detuning and dephasing that population inversion can no longer be accomplished. Furthermore, the phase of the pulse may become very relevant in determining the effectiveness of the pulse excitation, especially so the shorter the pulse is, whereas in the RWA or in the averaging approximation to 2nd-order, it plays no role. Examining Eqs. (28) one sees that if the detuning of the pulse is zero during the driving, then one could achieve population inversion. Based on this theoretical result, one could devise two strategies: one with chirped pulses that take into account the amplitude dependent

detuning of the Bloch-Siegert shift, and the other one with pulse shaping instead of chirping.

In the first strategy one could have a chirp on the pulse central frequency given by $\omega(t) = \omega_0 + \Omega_0(t)^2/\omega(t)$, hence the area theorem could be valid again. This should be the case, provided the time variation of $\omega(t)$ is not too fast. Next, we will use only the positive root of this quadratic equation, which is given by

$$\omega(t) = \frac{\omega_0 + \sqrt{\omega_0^2 + 4\Omega_0^2(t)}}{2}. \tag{29}$$

Furthermore, one needs $\Omega_0(t)$ to vary slowly in time compared with $2\pi/\omega_0$ and $\Omega_0(t) = O(\epsilon)$ and $\dot{\omega}(t) = O(\epsilon)$ at most, so that the averaging techniques can be applied. One should notice that when TLS's are driven by pulses, Floquet theory is not applicable, whereas averaging techniques may still be applied provided the above restrictions are maintained and that the transformation to a rotating frame is given by

$$\sigma(t) = e^{\imath \int_0^t \omega(s)ds} \tilde{\sigma}(t),$$

as was discussed in Ref. [20]. In order to achieve maximum population transfer, a Gaussian π-pulse should be given by

$$\begin{aligned} F(t) &= 2\Omega_0(t) \cos\left(\int_0^t \omega(s)ds + \varphi_0 \right) \\ &= 2\Omega_0 e^{-\frac{(t-t_0)^2}{2\sigma_0^2}} \cos(\omega_0 t + \varphi(t)), \end{aligned} \tag{30}$$

where the pulse instantaneous frequency $\omega(s)$ is given by Eq. (29) and $\sigma_0 = \dfrac{\sqrt{\pi}}{2\sqrt{2}\Omega_0}$ and $t_0 >> \sigma_0$.

In Fig. 4, one sees that this strategy yields very good results, with deep population inversions and little dependance on pulse carrier phase. Whereas, π-pulse excitations with central frequency $\omega = \omega_0$ yield results that are very dependent on pulse phase. This phase dependance becomes a more relevant issue the shorter the

pulse is. The drawback of this method is that it is likely not very easy to design the chirped pulses experimentally. In Fig. 5, with the presence of decoherence under the relaxation-time approximation the proposed strategy of using pulses with chirp yield deeper population invertions than what would be achieved with a resonant π-pulse excitation. One obtains a very good fit for the population inversion with the second-order averaging result and the numerics with pulse chirping.

The second strategy, though, involves no chirp, instead it keeps the effective detuning as small as possible by choosing the pulse maximum amplitude so that $\Omega_0 = \sqrt{\delta\omega}$. Here we need a near resonance condition of $\delta = \mathcal{O}(\epsilon^2)$, so that $\Omega_0 = \mathcal{O}(\epsilon)$, since $\omega = \mathcal{O}(1)$. Obviously, for this strategy to be valid, one needs a blue-shifted central frequency with respect to the transition frequency $\omega_0 = 1$ (in our units). The advantage of this method is that one can have an effective π-pulse even with a blue-shifted detuning, what is not possible when the McCall-Hahn's area theorem is valid, since it is based on the RWA.

In Fig. 6, we show a sequence of three Gaussian π-pulses each one with a central frequency of $\omega = 1.1$ and amplitude $2\Omega_0 = 0.2$ acting on the TLS. Due to the detuning almost only about 40% of the ground state population is excited after the three π-pulses. Both the RWA and averaging to 2nd-order predict well the behavior of the population after the first π-pulse, but break down afterwards as can be seen in frame (a). In frame (b) we show the instantaneous pulse shapes along with their envelopes and in frame (c) we show the accumulated area of the pulse envelopes as a function of time to attest that indeed we have π-pulses. One sees that if the pulse shape is not well chosen the π-pulses are not effective, the RWA and averaging approximation break down, and one loses quantum control over the qubit.

In Fig. 7, we again show a sequence of three Gaussian π-pulses, each one with a central frequency of $\omega = 1.1$ and envelope amplitude with $\Omega_0 = \sqrt{\delta\omega} = 0.331662$ acting on the TLS. One sees that due to the detuning, after three π-pulses the RWA

(red line) breaks down yielding less than 80% of population inversion. Whereas the averaging to 2nd-order still got approximately 98% of population inversion. With this value of pulse envelope amplitude, one achieves nearly 99% of population inversion by numerically integrating the density matrix equations of motion in Eqs. (21). This indicates that the averaging method to second-order is a good predictor of the behavior of the population transfer between the ground and excited levels when our pulse shaping strategy is implemented. In frame (b) we show the instantaneous pulse shapes along with their envelopes and in frame (c) we show the accumulated area of the pulse envelopes as a function of time to attest that indeed we have π-pulses.

In Fig. 8, we show a sequence of three Gaussian π-pulses each one with a central frequency of $\omega = 1.1$ and amplitude of twice $\Omega_0 = 0.5$ acting on the TLS. Due to the detuning almost only about 44% of the ground state population is excited after the three π-pulses. Both the RWA and averaging to 2nd-order break down as can be seen in frame (a). In frame (b) we show the instantaneous pulse shapes (with zero phase) along with their envelopes and in frame (c) we show the accumulated area of the pulse envelopes as a function of time to attest that indeed we have π-pulses. Again, one sees that if the pulse shape is not well chosen the π-pulses are not effective, the RWA and averaging approximation break down, and one loses quantum control over the qubit.

The results presented in Fig. 9 show the amount of population remaining in the ground state after a Gaussian π-pulse excitation is applied to the TLS. The shapes of the pulses in frames (a)-(c) are equal to the shapes of the the pulses in Figs. 6-8, respectively. In frame (a) there is no complete population inversion (under 80%) and the outcome of the pulse excitation depends considerably on the phase of pulse. Whereas, in frame (b), we notice that our pulse shaping strategy to generate the deepest inverstions works very well. Here, due to the Bloch-Siegert shift, the pulse is effectively in resonance, hence it is a π-pulse. We obtain very good fit with the

averaging and the numerical results with nearly complete inversion independent of pulse phase, what make performing quantum control of qubits is easier. In frame (c), since one gets again out of resonance due to the Bloch-Siegert shift, not only there is no complete population inversion, but there is also strong influence of the phase of the pulse on the outcome of the π-pulse excitation.

VI. CONCLUSION

Here we showed that perturbation techniques based on the averaging method can efficiently describe the unitary (or near unitary) time evolution of TLS's under coherent excitation. With the averaging method to second-order approximation, we went beyond the RWA in analyzing the dynamics of such a fundamental process in quantum mechanics. The numerical time-evolution of the ground state population of the TLS under cw driving had a far better fit with the averaging method to 2nd-order approximation than with the RWA time evolution. Basically, this better approximation was achieved by eliminating the dephasing that occurs in the RWA. By going to second-order in the averaging method, we obtained the Bloch-Siegert shift of the TLS resonant frequency, in which the resonant frequency increases quadratically with the driving field amplitude. This frequency shift is the main cause of the dephasing of the ground state population time evolution observed in the RWA.

Although, the proposed method is not exact as Floquet theory is in the case of cw driving of TLS's, it is far easier to implement than the latter theory. Furthermore, it can still be applied even when Floquet theory can no longer be applied, such as when the TLS is driven by short pulses.

We verified that the Bloch-Siegert frequency shift that occurs in cw driving, also has important influence on pulse-driven TLS's. This shift basically implies that the well-known area theorem of McCall and Hahn breaks down when the Rabi frequency

of pulse-driven TLS's becomes approximately of the order ($> 40\%$) of the transition frequency. By numerically integrating the optical-Bloch equations we note that, for intense and short π-pulse excitations, consistently more population inversion is achieved and with less phase dependance if the pulse central frequency has a chirp or the pulse amplitude is chosen so as to minimize the detuning effect of the Bloch-Siegert shift.

The present approaches of designing π-pulse shapes guided by the averaging method could be used in experimentally generating shorter π-pulses that achieve considerably more population inversion than with π-pulses without chirp or with the wrong shape. Our results may prove to be very helpful in speeding up control schemes of quantum qubits in quantum computation, since it minimizes the effects of pulse phase and decoherence on the effectiveness of the π-pulses. If one only achieves an imperfect population inversion, such as around 95% of inversion, after a few π-pulses one could lose the control over the qubits. The control of qubits for the realization of quantum gates is of fundamental importance in quantum computation [10], as they are usually realized by sequences of laser pulses in physical systems, such as, for instance, ion traps [21, 22]. It is important to mention that our methods are not restricted to the design of just the Gaussian-shaped π-pulses shown here, but they may be realized with other types of pulses used in the implementation of quantum gates. Furthermore, our results may prove to be useful for increasing the photocurrent in quantum dot (QD) devices [23] even when the pulse carrier frequency is not in resonance with the interlevel transition frequency of the QD.

Finally, we would like to point out that the fairly straight forward and powerful capabilities of the averaging method, such as those used here, should allow it to have a place among the usual time-dependent perturbative methods taught in standard

text books of quantum mechanics.

---

[1] J. Guckenheimer and P. Holmes, *Nonlinear Oscillations, Dynamical Systems, and Bifurcations of Vector Fields* (Springer-Verlag, New York, 1983).

[2] F. Verhulst, *Nonlinear Differential Equations and Dynamical Systems* (Springer-Verlag, New York, 1996).

[3] J. H. Shirley, Phys. Rev. B **138**, 974 (1965).

[4] H. Sambe, Phys. Rev. A **7**, 2203 (1973).

[5] F. Bloch and A. Siegert, Phys. Rev. **57**, 522 (1940).

[6] K. Bergmann, H. Theuer, and B. Shore, Rev. of Mod. Phys. **70**, 1003 (1998).

[7] M. Wollenhaupt, A. Präkelt, C. Sarpe-Tudoran, D. Liese, and T. Baumert, Appl. Phys. B **82**, 183 (2006).

[8] C. Trallero-Herrero and T. C. Weinacht, Phys. Rev. A **75**, 063401 (2007).

[9] C. Conover, Phys. Rev. A **84**, 063416 (2011).

[10] M. A. Nielsen and I. L. Chuang, *Quantum Computation and Quantum Information* (Cambridge University Press, 2010).

[11] S. L. McCall and E. L. Hahn, Phys. Rev. Lett. **18**, 908 (1967).

[12] S. L. McCall and E. L. Hahn, Phys. Rev. **183**, 457 (1968).

[13] L. Allen and J. H. Eberly, *Optical Resonance and Two-Level Atoms* (Dover, New York, 1987).

[14] J. Cao, C. J. Bardeen, and K. R. Wilson, Phys. Rev. Lett. **80**, 1406 (1998).

[15] S. Zamith, J. Degert, S. Stock, B. De Beauvoir, V. Blanchet, M. A. Bouchene, and B. Girard, Phys. Rev. Lett. **87**, 033001 (2001).

[16] P. K. Jha and Y. V. Rostovtsev, Phys. Rev. A **82**, 015801 (2010).

[17] I. I. Boradjiev and N. V. Vitanov, Phys. Rev. A **88**, 013402 (2013).

[18] I. I. Rabi, Phys. Rev. **51**, 652 (1937).

[19] A. A. Batista, B. Birnir, and M. S. Sherwin, Phys. Rev. B **61**, 15108 (2000).

[20] A. A. Batista and D. S. Citrin, Phys. Rev. Lett **92**, 127404 (2004).

[21] T. Monz, K. Kim, W. Hänsel, M. Riebe, A. Villar, P. Schindler, M. Chwalla, M. Hennrich, and R. Blatt, Phys. Rev. Lett. **102**, 040501 (2009).

[22] F. Schmidt-Kaler, H. Häffner, S. Gulde, M. Riebe, G. Lancaster, T. Deuschle, C. Becher, W. Hänsel, J. Eschner, C. Roos, *et al.*, Appl. Phys. B **77**, 789 (2003).

[23] A. Zrenner, E. Beham, S. Stuffler, F. Findeis, M. Bichler, and G. Abstreiter, Nature **418**, 612 (2002).

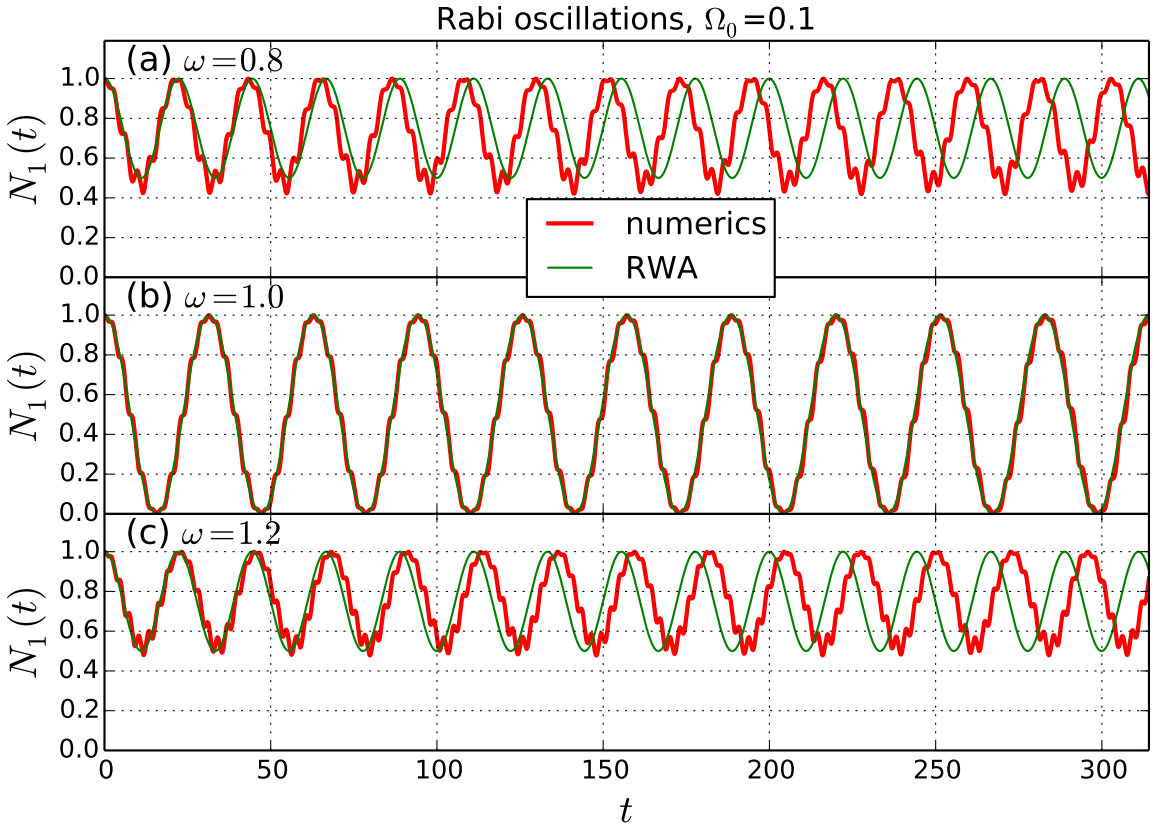


FIG. 1. Comparison of the ground state population time evolution as predicted by the RWA in Eq. (9) and the result given by numerical integration of Eqs. (3). In our units $\omega_0 = 1$.

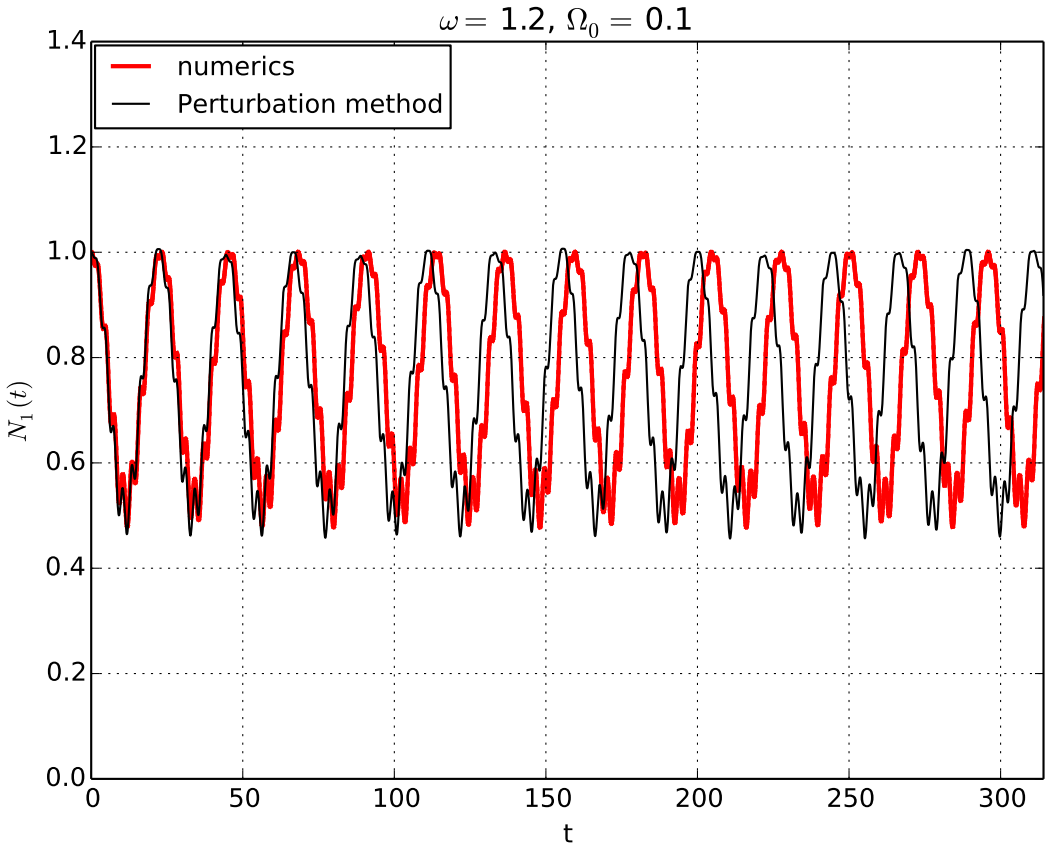


FIG. 2. Comparison of the ground state population time evolution as predicted by the naive perturbative method of Eq. (10) and the result given by numerical integration of Eqs. (3). Note that there is still the same problem of dephasing seen in Fig. (1), showing that this perturbative approach does not improve on the RWA.

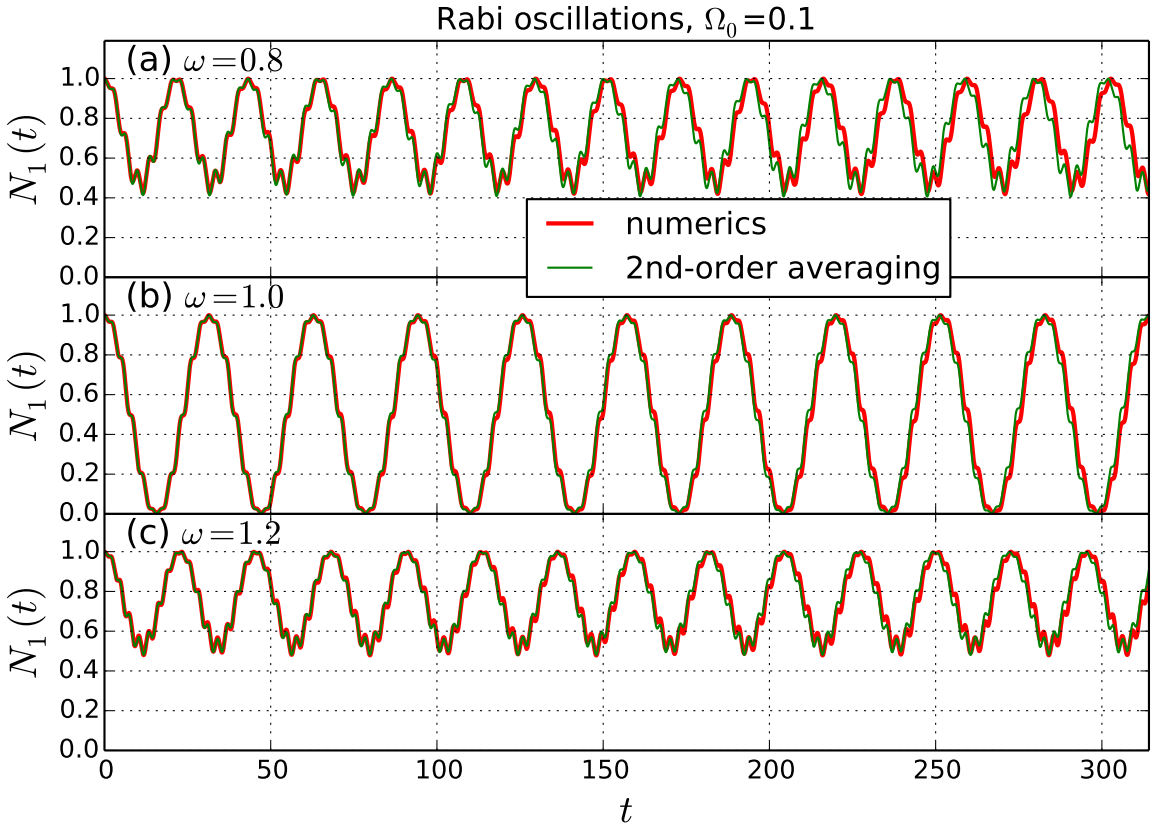


FIG. 3. Comparison of the ground state population time evolution as predicted by the 2nd-order averaging approximation of Eqs. (16) with the corrections of Eq. (14) and the result given by numerical integration of Eqs. (3). One can still see some dephasing, but it is far less pronounced than in the RWA results of Fig. 1.

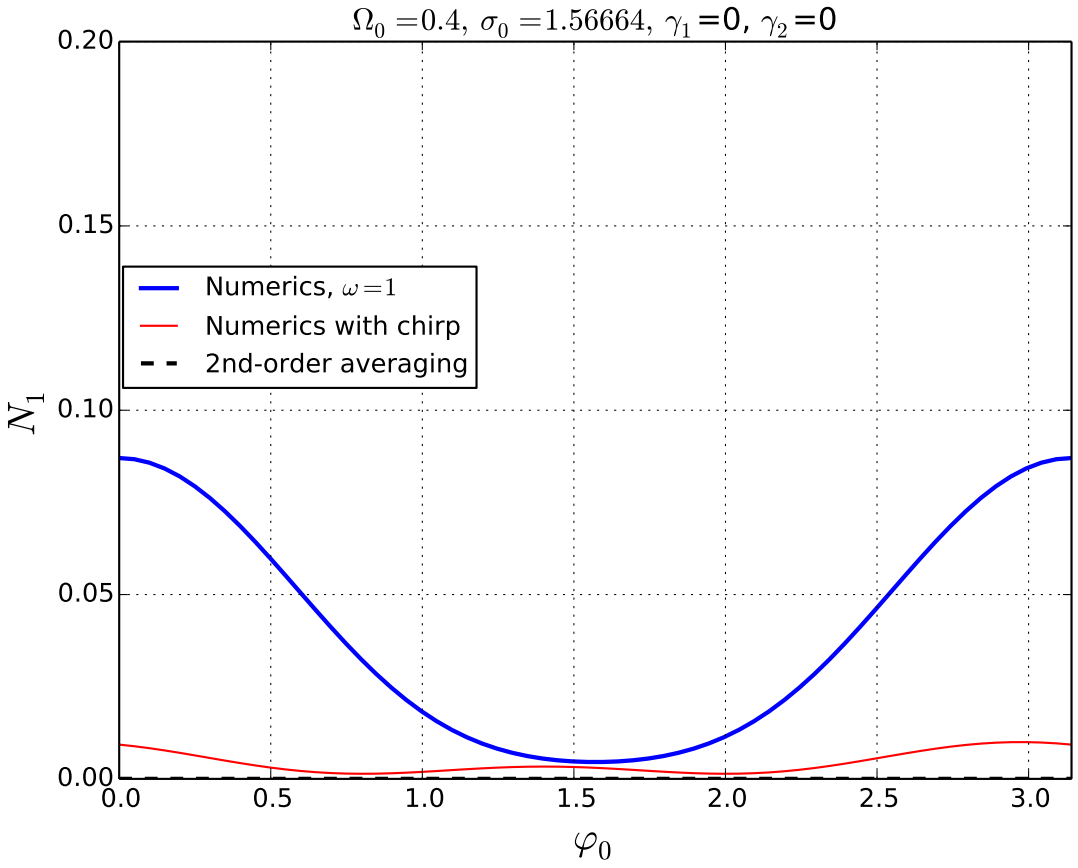


FIG. 4. Population in the ground level after a π-pulse excitation as a function of pulse carrier phase. Before the π-pulse excitation $N_1 = 1$. The thick blue line depicts the response due to a pulse without chirp, with central frequency $\omega = 1$, while the thin red line depicts the response to a chirped pulse with the central frequency $\omega(t)$ given by Eq. (29). The dashed black line is the corresponding 2nd-order averaging result, corresponding to an ideal population inversion independent of phase.

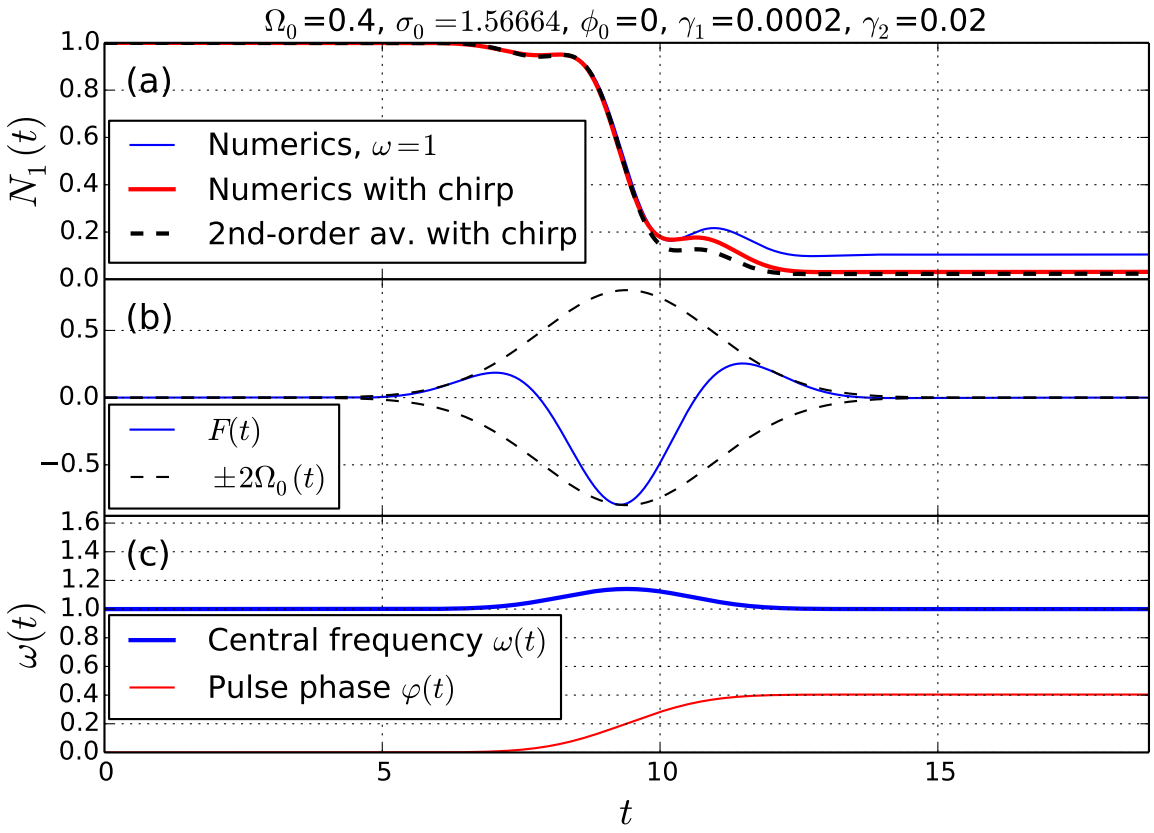


FIG. 5. Interlevel transitions driven by π-pulses with dissipation rates in the relaxation time approximation. In frame (a) we show the population of the ground level as a function of time. The thin blue line depicts the numerical result of the TLS excitation due to a pulse without chirp, with central frequency $\omega = 1$, the thick red line depicts the numerical results of the response to a chirped pulse with the central frequency $\omega(t)$ given by Eq. (29), and the dashed black line represents the corresponding averaged equations to second order with the corrections of Eq. (14) adapted to include chirp. In frame (b) we show the instantaneous chirped pulse along with the Gaussian envelope. In frame (c) we plot the central frequency and the pulse phase angle as a function of time.

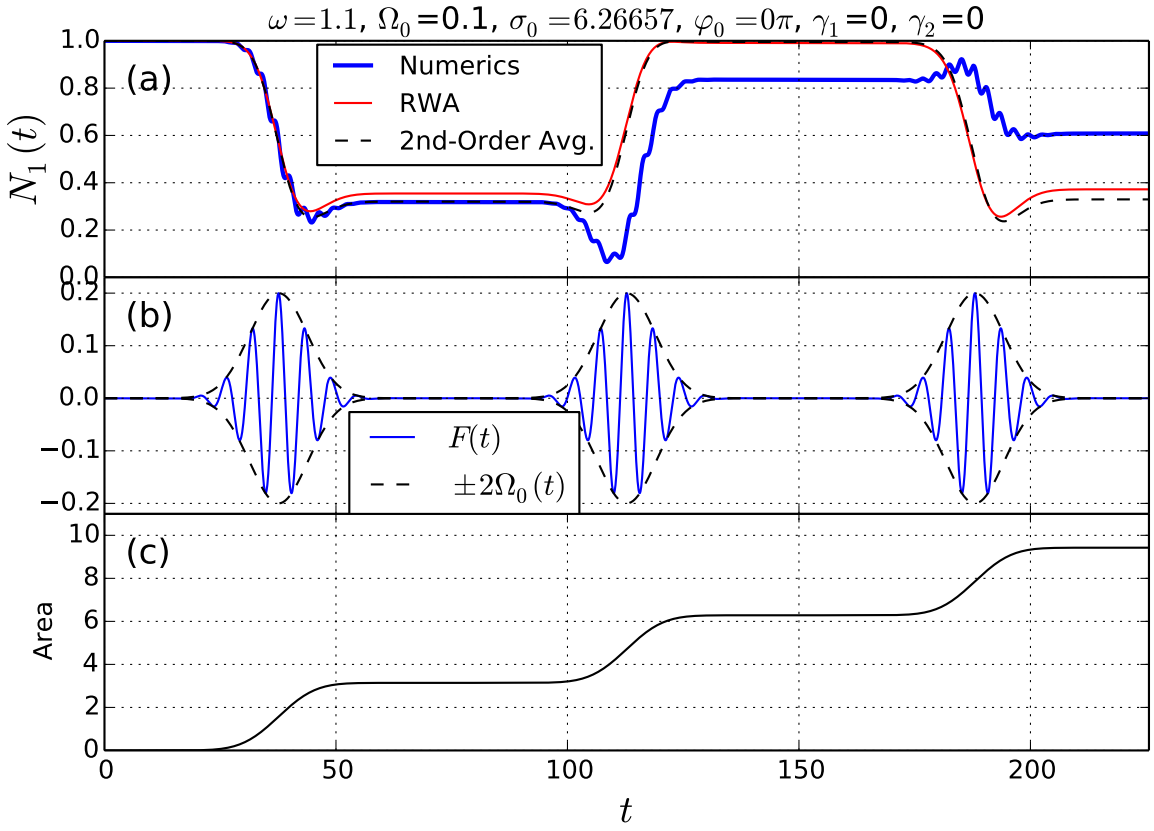


FIG. 6. Interlevel transitions driven by three π-pulses. In frame (a) we show the population of the ground level as a function of time. The excitations are pulses with carrier frequency at $\omega = 1.1$ and peak amplitudes with $\Omega_0 = 0.1$. The width and phase of the pulses are indicated in the figure. In frame (b) we show the instantaneous pulse shapes along with the π-pulse Gaussian envelopes. In frame (c) we plot the accumulated area of the pulse envelopes as a function of time, which shows that we actually have π-pulses.

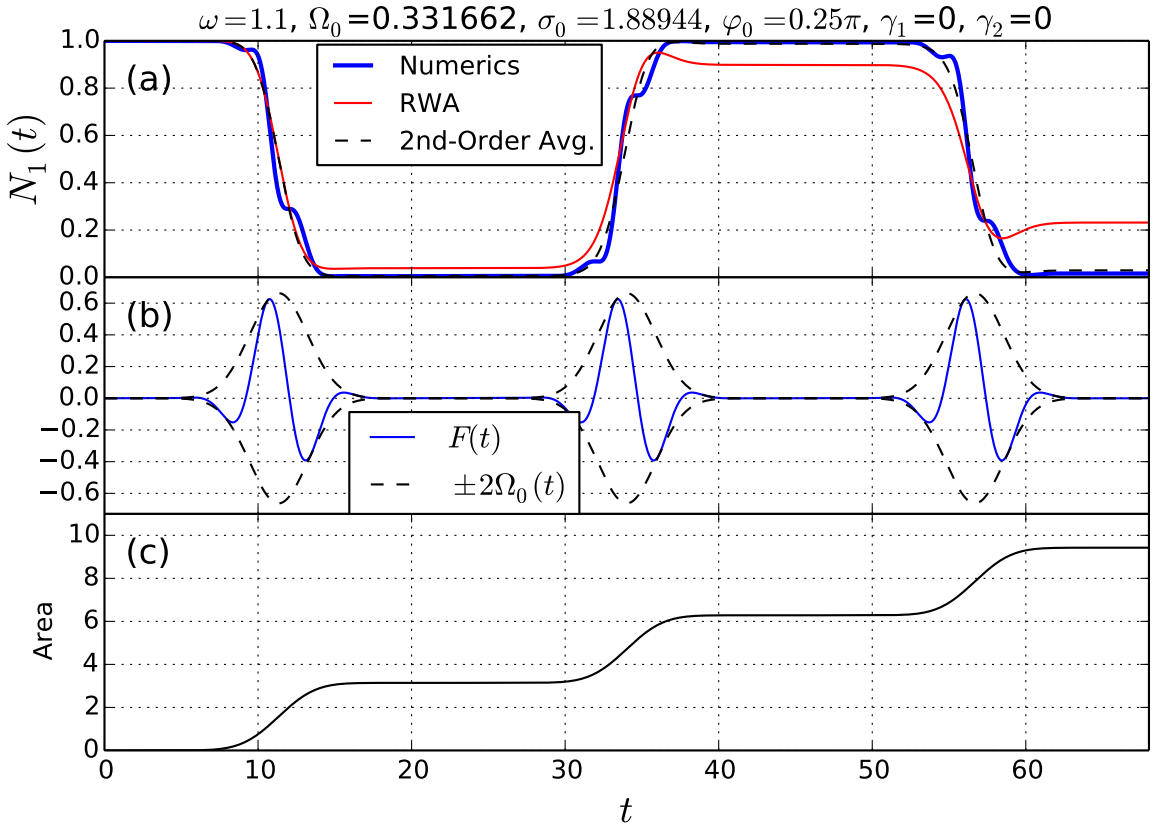


FIG. 7. Interlevel transitions driven by three π-pulses. In frame (a) we show the population of the ground level as a function of time. The thick blue line depicts the numerical integration result. One sees that complete population inversions are achieved, despite the fast dynamics, in which the RWA result (red line) is no longer valid. On the other hand, the results of the averaging method to second-order (dashed line) are still very useful in designing effective π-pulses. In frame (b) we show the instantaneous pulse shapes with central frequency at $\omega = 1.1$ along with the π-pulse Gaussian envelopes with peak amplitude with $\Omega_0 = \sqrt{\delta\omega}$. One sees that one gets about only one and a half cycles per pulse. In frame (c) one sees the accumulated area of the pulse envelopes as a function of time, at each pulse the area increases by π.

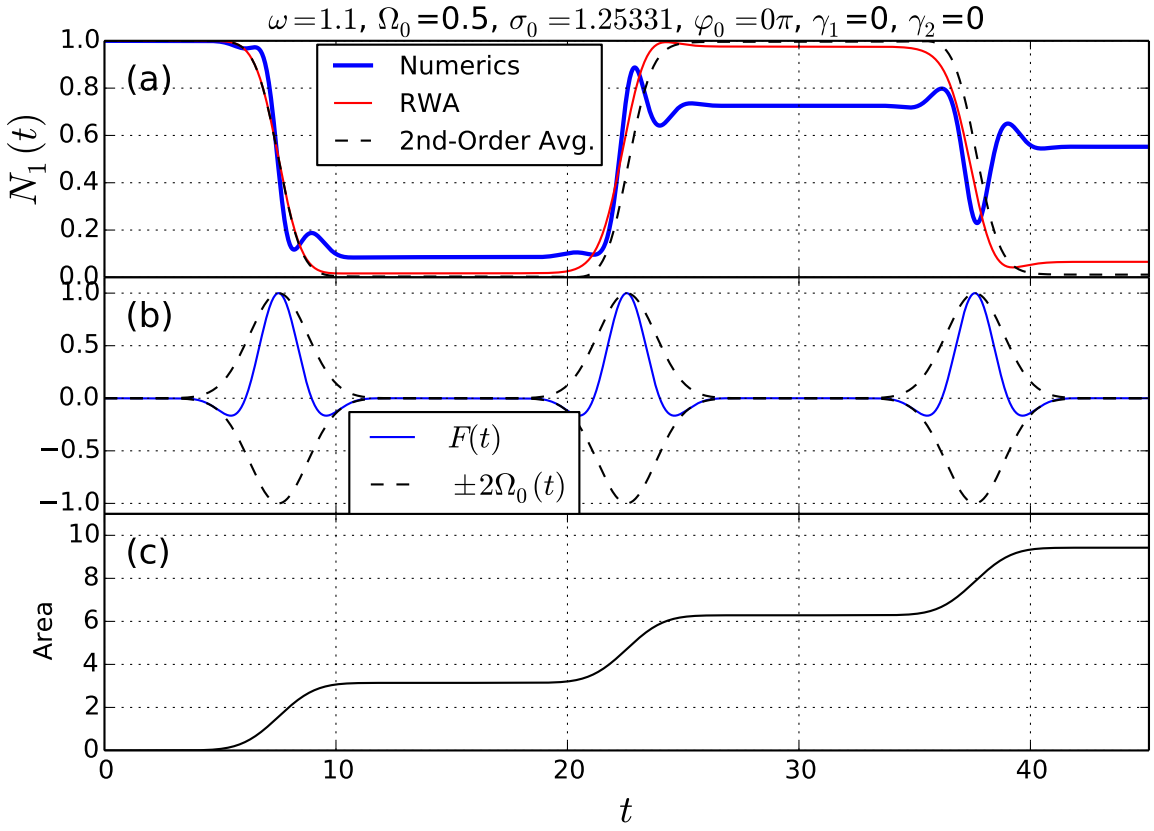


FIG. 8. Interlevel transitions driven by π-pulses. In frame (a) we show the population of the ground level as a function of time. The excitations are pulses with carrier frequency at $\omega = 1.1$ and peak amplitudes with $\Omega_0 = 0.5$. The width and phase of the pulses are indicated in the figure. The RWA and the averaging results both break down here. In frame (b) we show the instantaneous pulse shapes along with the π-pulse Gaussian envelopes. In frame (c) we plot the accumulated area of the pulse envelopes as a function of time, which verifies that we actually have π-pulses.

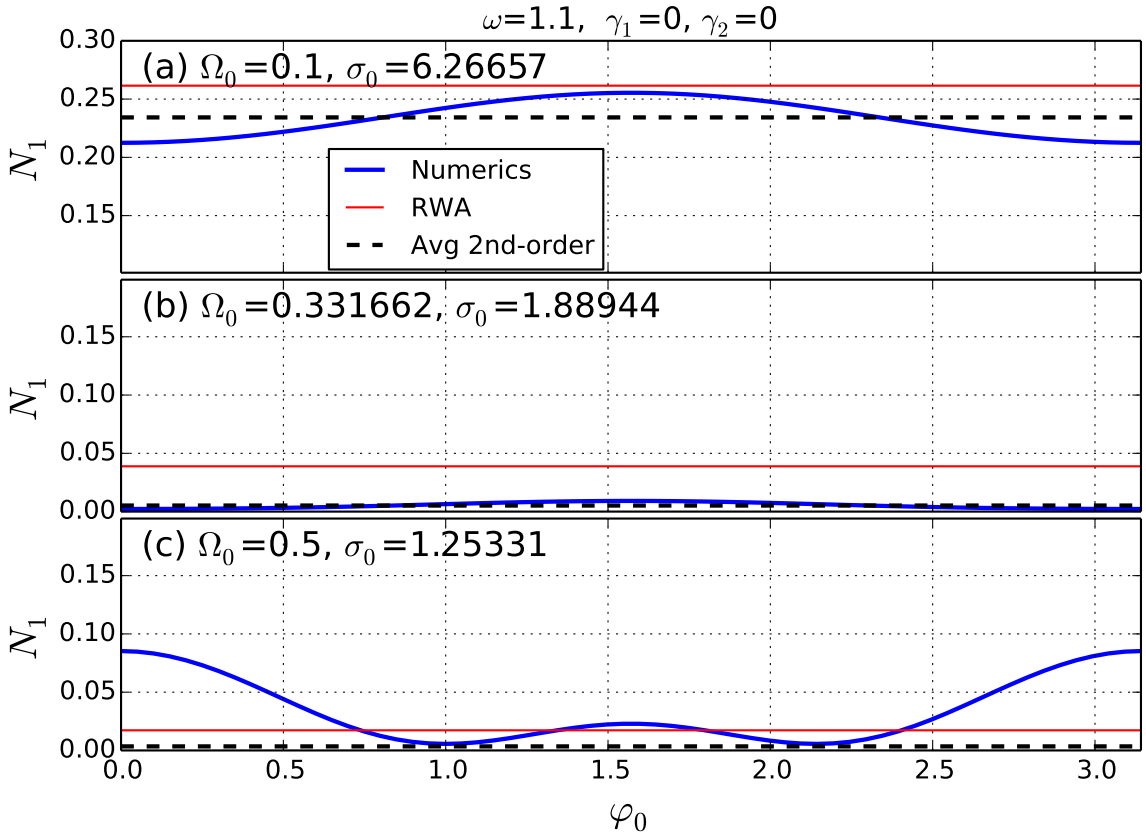


FIG. 9. Ground level population as a function of pulse phase after various π-pulse excitations with carrier frequency at $\omega = 1.1$. Note that before the excitation $N_1 = 1$ and that all pulse envelopes are Gaussian with amplitudes and widths indicated in each frame. In frame (a) we have dephasing due to the Bloch-Siegert shift and thus the outcome of the π-pulse is not a complete inversion and is very phase dependant. In frame (b) when the pulse amplitude is $2\Omega_0 = 2\sqrt{\delta\omega} \approx 0.6632$ the pulse is effectively at resonance, with nearly no dephasing due to the Bloch-Siegert shift. One sees that for this value of amplitude, one gets nearly complete inversion and very little phase dependance. This indicates that the pulse shaping procedure based on Eqs. (28), i.e. by keeping the detuning as low as possible, is very effective. In frame (c) we again have dephasing due to the Bloch-Siegert shift and thus the outcome of the π-pulse is very phase dependant.